Applied Catalysis B: Environmental 113–114 (2012) 107–115

Contents lists available at SciVerse ScienceDirect

Applied Catalysis B: Environmental

journal homepage: www.elsevier.com/locate/apcatb

Thermal effect of carboxylic acids in the degradation by photo-Fenton of high concentrations of ethylene glycol

J. Araña[a,b,*], J.A. Ortega Méndez[a,b], J.A. Herrera Melián[a,b], J.M. Doña Rodríguez[a,b], O. González Díaz[a,b], J. Pérez Peña[a,b]

[a] Grupo de Fotocatálisis y Electroquímica Aplicada al Medioambiente-FEAM (Unidad Asociada al Instituto de Ciencia de Materiales de Sevilla, C.S.I.C.) CIDIA-Dpto. de Química. Edificio del Parque Científico Tecnológico, Campus Universitario de Tafira, 35017, Las Palmas, Spain
[b] Universidad De Las Palmas De Gran Canaria, Las Palmas, Spain

ARTICLE INFO

Article history:
Received 8 August 2011
Received in revised form
11 November 2011
Accepted 15 November 2011
Available online 23 November 2011

Keywords:
Fenton
Photo-Fenton
Temperature
Complexes
Carboxylic acid
Ethylene glycol

ABSTRACT

The degradation by Fenton and photo-Fenton of high concentrations of ethylene glycol (1000–25,000 mg/L), similar to those found in wastewater has been studied. Strongly exothermic reactions led to temperature increments up to 70–94 °C. In most experiments, temperature increments favored radical formation that provided almost complete mineralization. Oxalic, formic and acetic acids were identified as degradation intermediates. The obtained results indicate that the radicals formed in the degradation of formic and acetic acids with H_2O_2 were responsible for the exothermic reactions. Nonetheless, Fe–oxalic complexes inhibited the previous reactions by slowing down the process in such a way that complete mineralization did not occur until those complexes were degraded.

FTIR studies allowed the identification of some of the complexes and species formed in the process.

1. Introduction

Nowadays, the proper management of industrial wastewaters is one of the important problems that modern societies must face. This generates environmental concern and supposes an important economic cost. The detoxification of most industrial wastewaters is not a simple task as it requires specific processes that depend on the type and concentration of the pollutants to be degraded. This is why the development of simple, economic processes capable of treating real, highly concentrated wastewaters is welcome.

Among the advanced oxidation technologies (AOTs), Fenton and photo-Fenton are characterized by their high efficiency and simple application. The main steps of these processes are the formation of •OH radicals from the reaction of Fe^{2+} with hydrogen peroxide (1) and from the photo-activation of the $Fe(OH)^{2+}$ complex (2) [1–4]:

$$Fe^{2+} + H_2O_2 \rightarrow Fe^{3+} + OH^{\bullet} + HO^{-} \quad (E_a = 39.5\,kJ/mol) \tag{1}$$

$$Fe(OH)^{2+} + h\nu \rightarrow Fe^{2+} + {}^{\bullet}OH (E_a = 11.4\,kJ/mol) \tag{2}$$

These apparently simple reactions require the control of different parameters to achieve high efficiencies. The numerous studies regarding their application to highly concentrated wastewaters have shown the complexity of these processes. Table 1 summarizes the values of the variables that control Fenton and photo-Fenton. As can be observed, though •OH radicals generated in reactions (1) and (2) do not react specifically, degradation efficiency and optimal H_2O_2/TOC (mol/mol) ratios depend on the nature of the sample. Many studies have shown that a high H_2O_2/TOC ratio notably reduces efficiency [7,10].

In addition to pH and the concentration of Fe^{2+} and H_2O_2, temperature is another parameter that controls reactions (1) and (2) but has not received much attention. It is known that the former reactions are endothermic [3,4] thus increasing temperature would produce more radicals. This has been shown for the treatment of 2,4-dichlorophenoxyacetic [15], phenolic mixtures [16] or paper pulp wastewater [8]. The main argument against using high temperatures in these processes is the faster H_2O_2 decomposition

* Corresponding author at: Grupo de Fotocatálisis y Electroquímica Aplicada al Medioambiente-FEAM (Unidad Asociada al Instituto de Ciencia de Materiales de Sevilla, C.S.I.C.) CIDIA-Dpto. de Química. Edificio del Parque Científico Tecnológico, Campus Universitario de Tafira, 35017, Las Palmas, Spain. Tel.: +34 928457299; fax: +34 928457397.
E-mail address: farana@dqui.ulpgc.es (J. Araña).

0926-3373/$ – see front matter © 2011 Elsevier B.V. All rights reserved.
doi:10.1016/j.apcatb.2011.11.025

Table 1
Variables of the application of Fenton and photo-Fenton to different wastewaters.

Waste	TOC or COD* (ppm)	H_2O_2 (g/L)	H_2O_2/TOC mol/mol	Degradation (%)
Polymers [5]	1100	17	5.49	100
Phenol [6]	1000	3.4	1.2	40
Municipal landfill [7]	3900	3.3	1.6*	30
Paper pulp [8]	525	10	6.7	70
Textile effluent [9]	600	10	5.8	8–70
Pulp mill [10]	110	1.7	5.2	85
Cork cooking [11]	1505	10	2.49	70
Pharmaceutical [12]	*7000**	170	–	100
Pharmaceutical [13]	*362,000**	102	–	55
Cosmetic	1090	9	2.9	60
[14]	705	12.7	6.37	48

* Chemical Oxygen Demand and italic values corresponding to COD.

into O_2 and H_2O [17]. However, it has been also shown that the presence of •OH radical scavengers reduces H_2O_2 thermal decomposition [15]. Other studies claimed that the efficiencies of Fenton and photo-Fenton at high temperature do not necessarily increase consumption of the oxidant [18].

In Fenton-like reactions, the formation of Fe^{2+} and/or Fe^{3+} complexes with reagents and/or intermediates reduces the efficiency of the process. For instance, the formation of a Fe(III)—*p*-hydroxybenzoic acid complex seems to be a key step to initiate its oxidizing mechanism [19]. The importance of complex formation has been revealed in the addition of phosphotungstate (PW12O40) that forms a soluble complex with iron that converts H_2O_2 into oxidants [20], tannic acid complexes in the degradation of polyphenols [21] or a citric acid complex in the degradation of dyes [22]. As observed with phenol, this effect is even more important at high concentrations of the organic pollutant [23].

Consequently, the present paper deals with the degradation of high concentrations of ethylene glycol by means of Fenton and photo-Fenton. Ethylene glycol is widely used in numerous industrial applications such as antifreeze agent in cooling and heating systems, in hydraulic brake systems, as ingredient in electrolytic condensers, as solvent in the paint and plastics industries, in inks for ball-point pens and printer's inks, in the manufacture of some synthetic fibers, in synthetic waxes, in some skin lotions and flavoring essences, in asphalt emulsion plants, in wood stains and adhesives and in leather dyeing and as de-icing fluid for airport runways. The concentrations of ethylene glycol in industrial wastewaters can reach 25–250 g/L. In lake waters, located close to places where ethylene glycol was used, concentrations as high as 19 g/L were measured [24,25].

The literature on the degradation of high concentrations by TAOs of ethylene glycol is scarce. Dietrick McGinnis et al. [26,27] studied the degradation of 1000 ppm of ethylene glycol, which is a much lower concentration than those found in actual industrial wastewaters. Thus, the present paper deals with the optimization of the treatment of higher concentrations of the organic pollutant by means of Fenton and photo-Fenton and the identification of the reactions involved.

2. Experimental

2.1. Material

The concentration of ethylene glycol (99% Panreac, Spain) in the degradation experiments ranged between 1000 and 25,000 ppm. Ethylene glycol (CH_2OH–CH_2OH) is characterized by being soluble in water in all proportions. In addition to the results shown in this work, experiments with real wastewaters (spent car radiator liquid) were performed with the same TOC concentrations. BOD and COD initial values were from 900–22,500 to 1537–38,425 g/L respectively. The results obtained with the real wastewater have been similar to those with ethylene glycol and are not shown.

For Fenton and photo-Fenton reactions, high purity $FeSO_4{\cdot}7H_2O$ (Panreac, Spain) and 35% (w/v) H_2O_2 from Scharlau were used. All the experiments were performed without aeration and at pH 3 without any noticeable change along the experiments. When was necessary, the initial pH was adjusted with H_2SO_4 (95–97% Scharlau).

All the reactions were performed with 200 mL of samples in cylindrical glass reactors (diameter: 5 cm, depth: 20 cm).

2.2. Equipment and techniques

A 60 W Solarium Philips HB175 equipped with four 15 W Philips CLEO fluorescent tubes with emission spectrum from 300 to 400 nm (maximum around 365 nm) was used as UV source in photo-Fenton experiments.

Toxicity was determined by means of the *Lemna minor* toxicity test [28]. Glass Petri dishes containing 13 ± 2 fronds of common duckweed (*L. minor*) were placed under constant visible radiation (one 18-W fluorescence tube placed approximately 25 cm above the test chambers) for 96 ± 2 h in a chamber with an ambient temperature of $23 \pm 1\,^{\circ}C$. Four replicates were used for each sample, i.e., a control without pollutant and samples taken at different reaction times or pollutant concentrations. To 50 mL of solution (pollutant aliquots and control), 15 drops of each concentrated nutrient solution (A–C) were added. To each dish 10 mL of sample at pH 7.5–8 were added. Growth inhibition percentage (I) was calculated with respect to the control without pollutant according to:

$$I(\%) = \left(\frac{C - T}{C}\right) \times 100$$

where *C* and *T* are the frond number mean increments for the control and the sample, respectively.

TOC (total organic carbon), TC (total carbon) and IC (inorganic carbon) were measured with a TOC Shimadzu 5000-A. A Thermo Heλios UV–vis spectrophotometer was used for spectra acquisition.

A Dionex ion chromatography (column: Ion PAC AS11-HC, mobile phase: 30 mM NaOH and suppressed conductivity ASRS-ULTRA) was used for the analysis of the carboxylic acids produced in the degradation experiments.

The remaining concentrations of H_2O_2 at different reaction times were HPLC-measured using a Supelco Discovery C18 25 cm × 4.6 mm ID, 5 μm particles column and an acetonitrile–water (20:80) as mobile phase, using a UV detector (λ = 210 nm).

3. Results and discussion

3.1. Toxicity results

From the economic viewpoint, biological methods are the most appropriate for wastewater treatment. Nevertheless, their application is restricted to samples with low toxicity and high biodegradability. Consequently, the first step of this research was to evaluate the toxicity of pure ethylene glycol in water and spent car radiator liquid (Fig. 1). As can be observed, the results for both samples are similar, indicating that toxicity was attributable almost only to ethylene glycol. At concentrations below 3000 ppm, a negative growth inhibition was obtained. This means that the plants can be using the pollutant as a nutrient to grow faster than the control without ethylene glycol. At concentrations greater than 5000 ppm, *L. minor* growth inhibition was greater than 50% and achieved 100% with 10,000 ppm. Other authors have indicated that the toxic thresholds of this compound for microorganisms are above 1000 ppm. EC50s for growth in microalgae are 6500 ppm or

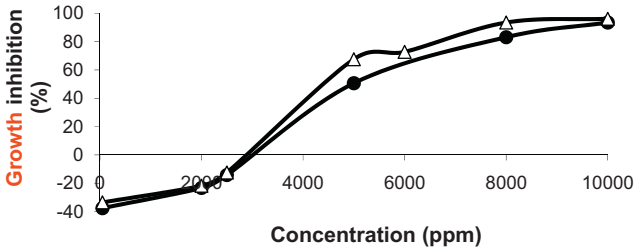

Fig. 1. Toxicity towards *Lemna minor* of pure aqueous ethylene glycol (Δ) and ethylene glycol-based spent car radiator liquid (●).

higher (similar to the indicated in Fig. 1). Acute toxicity tests with aquatic invertebrates revealed an LC50 s above 20,000 ppm, and those with fish provided LC50 s above 17,800 ppm [29]. Though ethylene glycol is not particularly toxic, it can withdraw high amounts of dissolved oxygen from the receiving streams leading to anoxia and eutrophication.

As a consequence, the toxicity and high dissolved oxygen demand of ethylene glycol concentrations above 5000 ppm make their aerobic treatment a hard task. These results support the interest of optimizing the treatment of high concentrations of ethylene glycol.

3.2. Fenton of ethylene glycol

The first Fenton experiments were performed with a TOC concentration of 10,650 ppm, varying the initial concentration of H_2O_2 ([H_2O_2]) between 15 and 120 g/L and a constant concentration of Fe^{2+} (200 ppm) (Fig. 2). After 100 h of reaction, the TOC of the experiments with the highest concentration of the peroxide (90 and 120 g/L) was reduced down to less than 1300 ppm.

These experiments were repeated with Fe^{2+} concentrations varying between 50 and 800 ppm and keeping H_2O_2 concentration constant in 90 g/L. At concentrations below 200 ppm, the efficiency was notably lower while at higher concentrations no significant efficiency improvement was achieved. Thus, for the following experiments Fe^{2+} concentration was 200 ppm.

Fenton experiments with lower ethylene glycol concentrations (1000 ppm of TOC) were also performed by varying the concentration of H_2O_2. Fig. 3 shows the results obtained with 10,000 and 1000 ppm as a function of the H_2O_2/TOC (mol/mol) ratio. For both

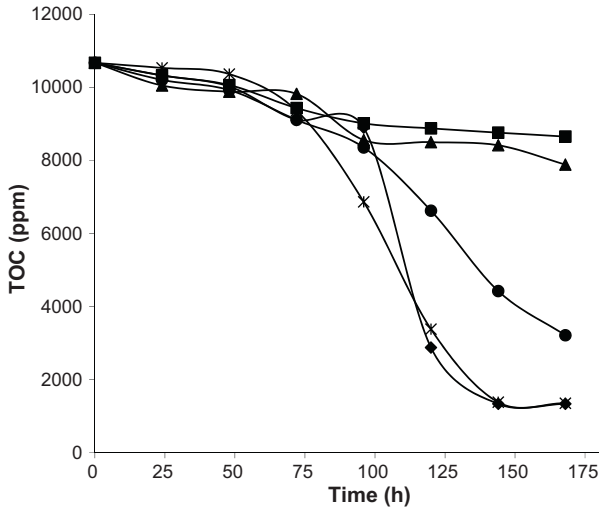

Fig. 2. Ethylene glycol mineralization by Fenton varying [H_2O_2]: ■ 15, ▲30, ●60,♦ 90 and Ж 120 g/L [Fe^{2+}] = 200 ppm.

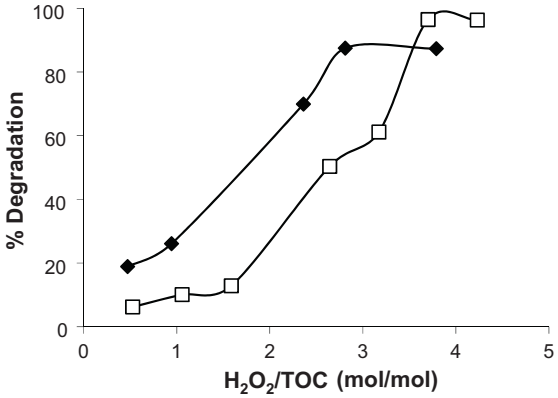

Fig. 3. Mineralization achieved (%) of 10,000 ppm of ethylene glycol after 168 h (♦) and 1000 ppm after 48 h (□) by Fenton varying the mol/mol [H_2O_2]/[TOC] ratio [Fe^{2+}]: 200 ppm.

concentrations, degradation was above 60% only when the ratio was greater than 3.

Though the obtained results were promising, the reaction time was too long. Thus, with the goal of improving the degradation process, the following experiments were performed:

- Different samples with initial TOC between 10,000 and 18,000 ppm were treated by means of Fenton with 200 ppm of Fe^{2+} and 90 g/L of H_2O_2 for 8, 12, 24 and 72 h.
- After this, to the so treated samples, 200 ppm of Fe^{2+} were added again and irradiated.

The obtained results are shown in Fig. 4. In all cases, after the second addition of Fe^{2+} and irradiation, temperature was increased up from 32.5 °C to 94 °C and the total mineralization was achieved in less than 1 h of irradiation. At the end of the process a yellow precipitate was formed. The strong mineralization achieved (as high as 14,000 ppm in less than 1 h) after the addition of iron and irradiation of the samples implies the presence of reactions none described until now in the literature for these techniques.

3.3. Photo-Fenton of ethylene glycol

To better understand the degradation mechanisms of the reactions observed in the studies previously described, the direct photo-Fenton degradation of ethylene glycol samples with TOC concentrations ranging between 350 and 11,000 ppm was

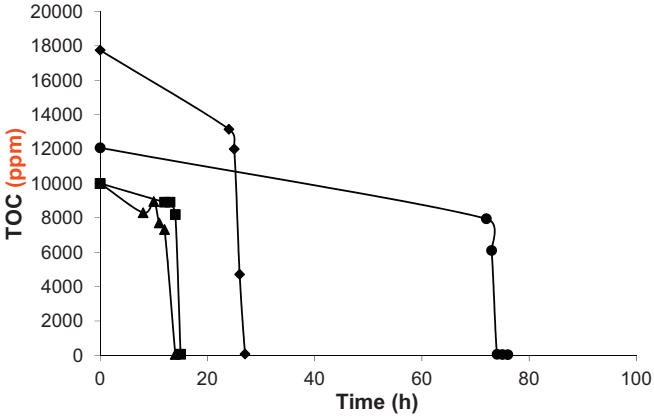

Fig. 4. Effect of irradiation and the new addition of Fe^{2+} after different Fenton reaction times: 8 h (▲), 12 h (■), 24 h (♦) and 72 (●).

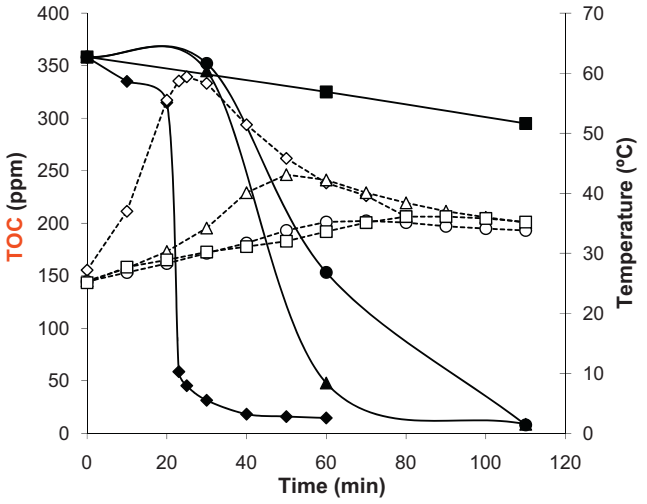

Fig. 5. Evolution of TOC (full symbols) and temperature (empty symbols) during the degradation of 350 ppm of ethylene glycol with different [H_2O_2]: 15 ■ □, 30● ○, 60▲△ and 120 ♦ ◊ g/L.

performed. Figs. 5 and 6 show the evolution of TOC, temperature and concentrations of acids identified (formic, acetic and oxalic) as intermediates for the experiments performed with 350 ppm of TOC from ethylene glycol. The concentration of Fe^{2+} was 200 ppm and that of H_2O_2 was varied between 15 and 120 g/L.

Mineralizations were very low with the lowest concentrations of H_2O_2 (15 and 30 g/L). However, the concentration of the acids was high after 60 min, (Figs. 5 and 6). Faster mineralization was achieved with higher concentrations of the peroxide but after a lag phase in which it was very slow. This behavior was observed more clearly with the highest concentration of H_2O_2 employed (120 g/L). In this case mineralization after the first 20 min was 12% but after 30 min was 91.3%. As indicated above, temperature was monitored (Fig. 5) being exponentially increased just before the rapid TOC reduction. This temperature increment (ΔT) was greater and appeared earlier with increasing concentrations of H_2O_2.

The global Fenton and photo-Fenton process is exothermic. Nonetheless, the ΔT obtained with 120 g/L of H_2O_2 and ethylene glycol (350 ppm Fig. 5) was notably greater than those of the blank experiments (without organic matter, Fig. 7). In addition to this, the ΔT of the reactions with lower concentrations of the peroxide and ethylene glycol was slightly lower and appears at the same time than that of the photo-Fenton blank study.

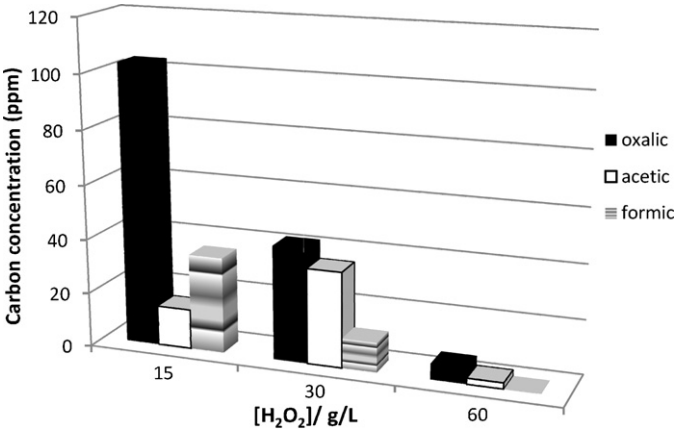

Fig. 6. Concentrations of carbon of the acids after 60 min of photo-Fenton during the degradation of 350 ppm of ethylene glycol with different [H_2O_2].

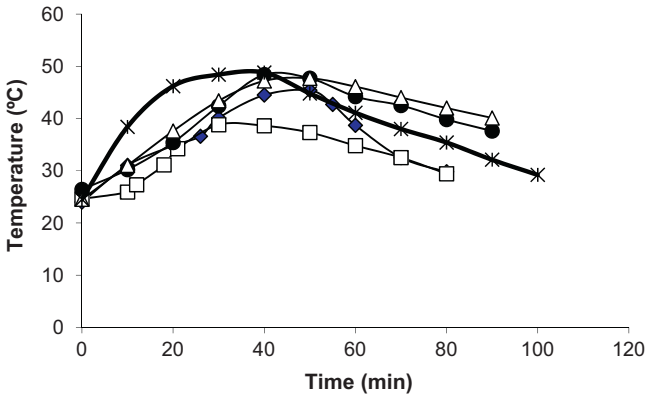

Fig. 7. Blank experiments (in the absence of organic matter) for Fenton (Ж 120 g/L of H_2O_2) and photo-Fenton with different concentrations of H_2O_2: □ 15, ♦ 30, ● 60 and △ 120 g/L [Fe^{2+}]: 200 ppm.

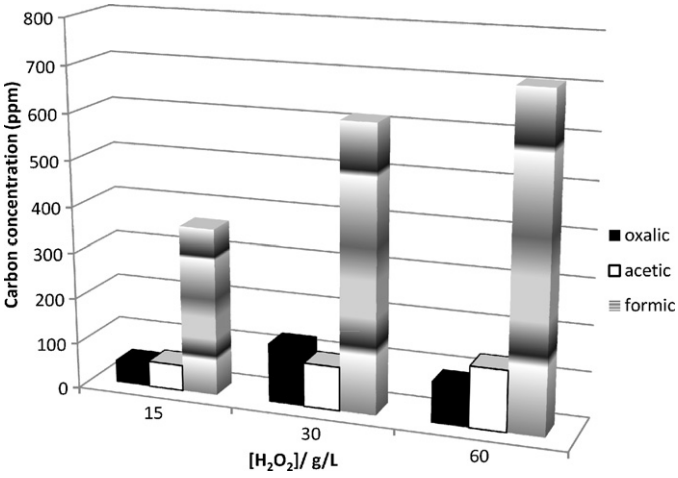

Fig. 8. Concentration of carbon of the acids after 240 min of photo-Fenton reaction of 11,600 ppm of ethylene glycol de ethylene glycol (as TOC) at different concentrations of H_2O_2 [Fe^{2+}]: 200 ppm.

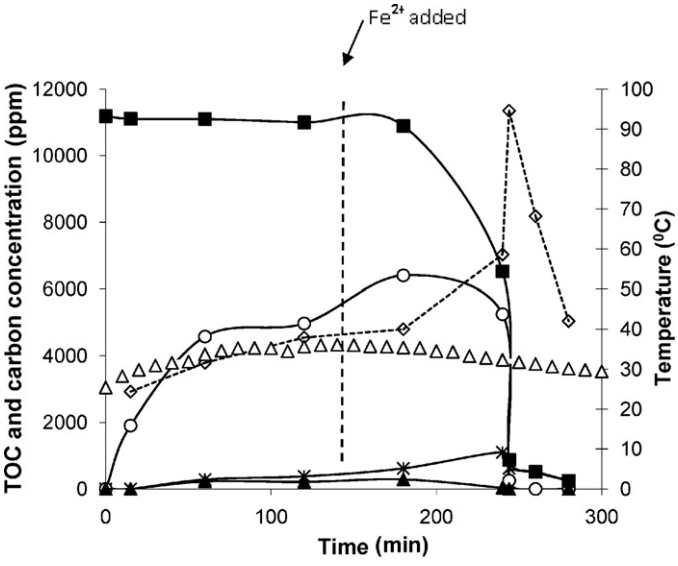

Fig. 9. Photo-Fenton degradation of 11,600 ppm of ethylene glycol (as TOC). Evolution of: intermediates (as carbon concentration) (○ formic, ▲oxalic and Ж acetic acid) and temperature (◊) with [H_2O_2]: 120 g/L and [Fe^{2+}]: 200 ppm. After 150 min, other 200 ppm of Fe^{2+} was added. The evolution of temperature in the experiments performed with aeration is also shown (Δ).

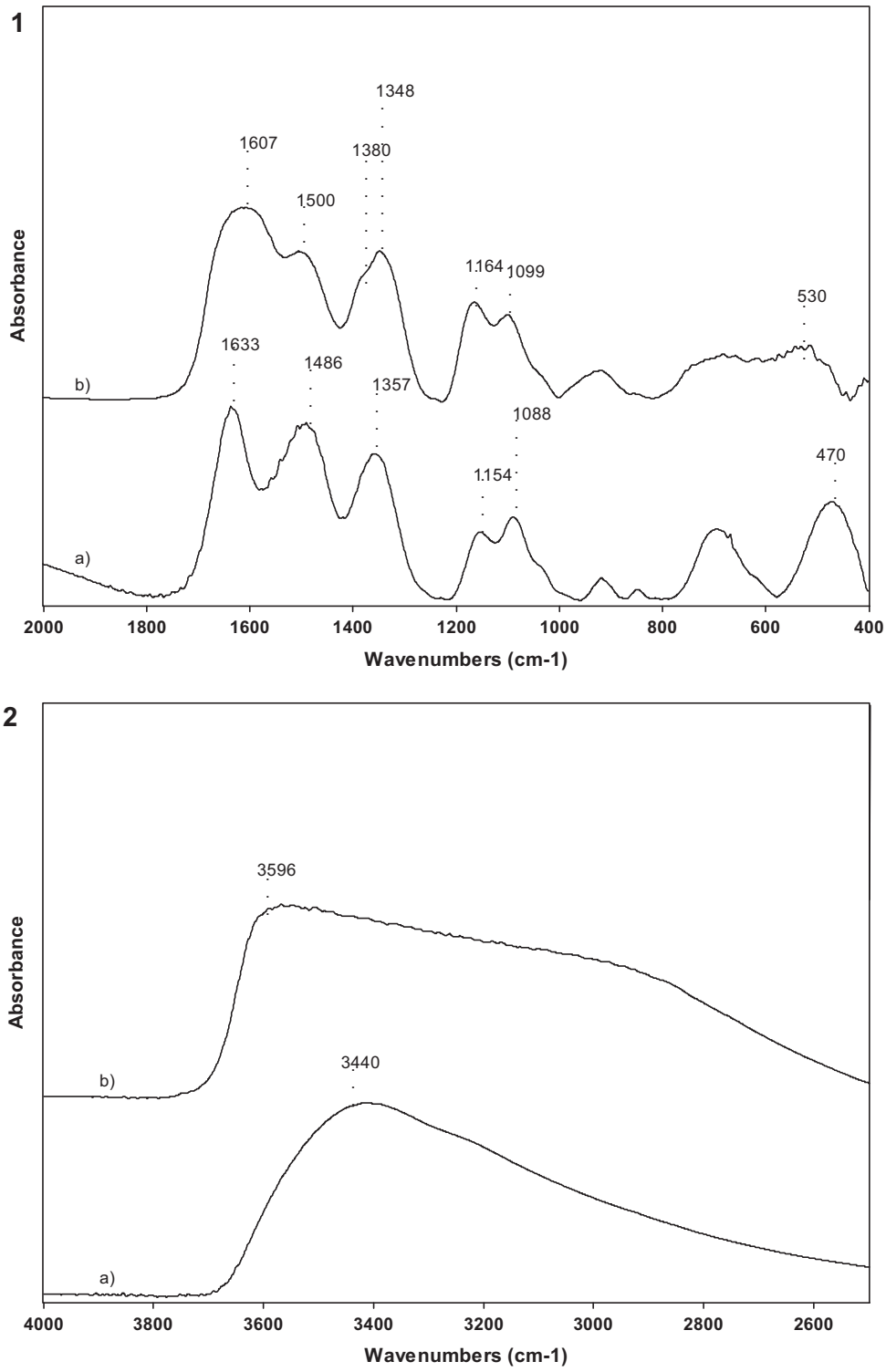

Fig. 10. (1) FTIR spectra from the solid formed in the degradation of 11,600 ppm of TOC of ethylene glycol by photo-Fenton in the region between 2000 and 400 cm^{-1}, after the total mineralization (a) and after 200 min of reaction, just before the exponential ΔT (b). (2) FTIR spectra from the solid formed in the degradation of 11,600 ppm of TOC of ethylene glycol in the region between 4000 and 2500 cm^{-1}, after the total mineralization (a) and after 200 min of reaction just before the exponential ΔT (b).

In the experiments with Fenton and photo-Fenton, the addition of H_2O_2 darkened the solution's color to become brown-reddish. As the reaction progressed, the color changed to orange–yellow. The brown color is attributed to Fe^{3+} ions formed in the Fenton reaction, which is characterized by being fast and endothermic (1). The orange-yellowish color is attributed to the goethite produced by reaction (3), which is much slower and endothermic than reaction (1) and comprises various steps [30]. The first step that leads to the formation of $FeOOH^{2+}$ (reaction (3.1)) is favored by incremented concentrations of H_2O_2. The formation of $HO_2^{\bullet}$ by means of reaction (3.2) is notably slower. The production of $HO_2^{\bullet}$ radicals is three times more endothermic than that of $^{\bullet}OH$ radicals by the

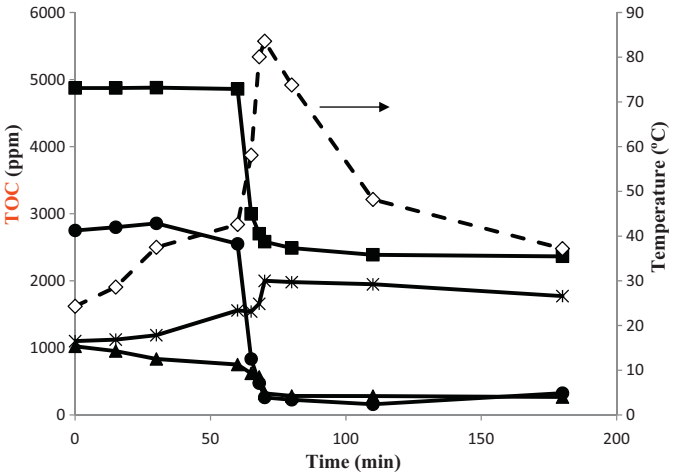

Fig. 11. Evolution of total TOC (■), formic (●), acetic (Ж) and oxalic (▲) acids and temperature (◊) during the photo-Fenton degradation of a mixture of the three acids. [H_2O_2]: 120 g/L, [Fe^{2+}]: 200 ppm. The concentrations of carboxylic acids are provided as TOC.

Fenton reaction (1) [3,31,32]

$$Fe^{3+} + H_2O_2 \rightarrow Fe^{2+} + HO_2^{\bullet} + H^+ \quad (k = 0.01\text{–}0.02\,M^{-1}\,s^{-1})\,E_a = 126\,kJ/mol \tag{3}$$

$$Fe^{3+} + H_2O_2 \leftrightarrow FeOOH^{2+} + H^+, \quad (K_{eq} = 3.1 \times 10^{-3}) \tag{3.1}$$

$$Fe - OOH^{2+} \rightarrow HO_2^{\bullet} + Fe^{2+} \quad (k = 2.7 \times 10^{-3}\,s^{-1}) \tag{3.2}$$

Under irradiation, the endothermic reaction (2) also occurs.

During the blank studies, the concentration of H_2O_2 was progressively diminished as temperature was increased. This can be attributed to the peroxide reaction with the generated radicals according to reactions (4) and (5), though they can react among them to yield H_2O_2 (6) or H_2O (7) [33–35].

$$H_2O_2 + HO^{\bullet} \rightarrow HO_2^{\bullet} + H_2O \quad (k = 3.3 \times 10^7\,M^{-1}\,s^{-1})\,E_a = 14\,kJ/mol \tag{4}$$

$$H_2O_2 + HO_2^{\bullet} \rightarrow HO^{\bullet} + H_2O + O_2 \tag{5}$$

$$2HO_2^{\bullet} \rightarrow H_2O_2 + O_2 \tag{6}$$

$$HO_2^{\bullet} + HO^{\bullet} \rightarrow H_2O + O_2 \tag{7}$$

$$OH + {}^{\bullet}OH \rightarrow H_2O_2 \tag{8}$$

Among reactions (5)–(7) there must be other one or more highly exothermic reactions that would be responsible for the observed ΔT that provide the necessary heat for reactions (1)–(4).

In addition to this, ΔT for the blank reaction (in Fenton) was faster than that under UV radiation. Radiation favors reaction (2) whose E_a is 11 times lower than that of reaction (3). If reaction (3) is inhibited the production of $HO_2^{\bullet}$ radical would be reduced and reactions (5)–(8) would become hampered. As stated above, these reactions are considered to be responsible for ΔT.

In addition to this, ΔT for the reactions performed with ethylene glycol and 120 g/L H_2O_2 was significantly higher than that of the blank studies. Thus, in that case in addition to reactions (1)–(8), the degradation of the organic compounds occurred:

$$ROH + {}^{\bullet}OH \rightarrow RO^{\bullet} + H_2O \tag{9}$$

$$R\text{–}COOH + {}^{\bullet}OH \rightarrow R\text{–}COO^{\bullet} + H_2O \rightarrow R^{\bullet} + CO_2 + H_2O \tag{10}$$

$$R^{\bullet} + O_2 \rightarrow ROO^{\bullet} \tag{11}$$

$$HO_2^{\bullet} + Fe^{3+} \rightarrow Fe^{2+} + H^+ + O_2 \tag{12}$$

$$R\text{–}COO^{\bullet} + H_2O_2 \rightarrow R\text{–}COOH + HO_2^{\bullet} \tag{13}$$

Degradation processes through •OH radical attack have been considered to be endothermic [36]. In fact, in the experiments with H_2O_2 concentrations of 15 and 30 g/L the observed ΔT was lower than those of the blanks (Fig. 5), most probably being the heat consumed by reactions (9) and (10).

Nonetheless, one of the reactions (11)–(13) must be highly exothermic to justify the observed ΔT (Fig. 5). Since the highest peroxide concentrations provided the strongest ΔT, it is probable that reaction (13) was the main responsible for it. Such ΔT favors reactions (1)–(3) and mineralization, as well.

Additionally, a solution of ethylene glycol of 30 g/L (11,600 ppm of TOC, i.e., similar concentrations than those present in wastewaters that contain the organic pollutants), was treated by photo-Fenton. At concentrations of hydrogen peroxide between 15 and 60 g/L, no mineralization but degradation (Fig. 8) was observed. Formic acid was the intermediate of highest concentration but acetic and oxalic acids were also detected. The evolution of temperature was similar to that of the experiments with 1000 ppm of ethylene glycol and concentrations of H_2O_2 of 15 and 30 g/L. Nonetheless, in the experiments performed with 120 g/L of H_2O_2 (Fig. 9) almost no mineralization was achieved during the first 120 min of reaction. However, similarly to the observed with lower concentrations of peroxide, notably high concentrations of intermediates (formic, acetic and oxalic acids) were found. The concentrations of the acids remained almost constant after the first 60 min of reaction. After 150 min, Fe^{2+} (200 ppm) was added again. During the following minutes, temperature and the concentrations of formic and acetic acids became progressively increased and that of oxalic reduced. Later, temperature augmented rapidly up to 94.6 °C and almost complete mineralization was achieved in about 5 min.

Lower ΔT (72 °C) than those observed in this study were obtained in Fenton experiments with higher concentrations of H_2O_2 (433.5 g/L) in the presence of acetic acid (3.75 M) [37]. The results obtained in the present study have shown that ΔT is correlated with the increment of the concentrations of formic and acetic acids. In fact, the greater ΔT have been observed with the highest concentrations of such acids and that of oxalic was the lowest. Dietrick McGinnis et al. [27,28] did not indicate any temperature change with concentrations of ethylene glycol of 1000 ppm, similar to those shown in Fig. 5. Nevertheless, they used lower concentrations of H_2O_2 and the mineralizations they achieved were not as high as those found in this study.

As indicated above, several works have shown that higher temperatures speed up photo-Fenton reaction [8,9]. As indicated above, reactions (1)–(3) are endothermic being thus prompted by higher temperatures. In fact, similar essays have been performed in the absence of UV radiation but incrementing temperature by heating and the same mineralization results have been achieved. This confirms the efficiency of increasing temperature in these processes.

At this point it must be indicated that after the exponential ΔT and almost complete mineralization, a yellowish precipitate was observed. The precipitate was studied by FTIR (Fig. 10 1). The bands observed are attributed to the following vibrations: δ(OH) (1486 and 1357 cm^{-1}), γ(OH) (698 cm^{-1}) and ν(FeO) (470 cm^{-1}) for FeOOH [38]. A less abundant solid that appeared in the solutions a few minutes before the ΔT was also analysed (Fig. 10 2). The spectrum is characterized by the following details: the bands corresponding to vibrations δ(OH) and ν(FeO) from FeOOH are shifted (1500 and 1348 cm^{-1} and 530 cm^{-1}, respectively), new bands appear at 1607 and 1380 cm^{-1} that are attributed to Fe–formic acid complexes [39]. In addition to this, the vibration bands attributed to stretching and bending overtone of H_2O_2 and water and those

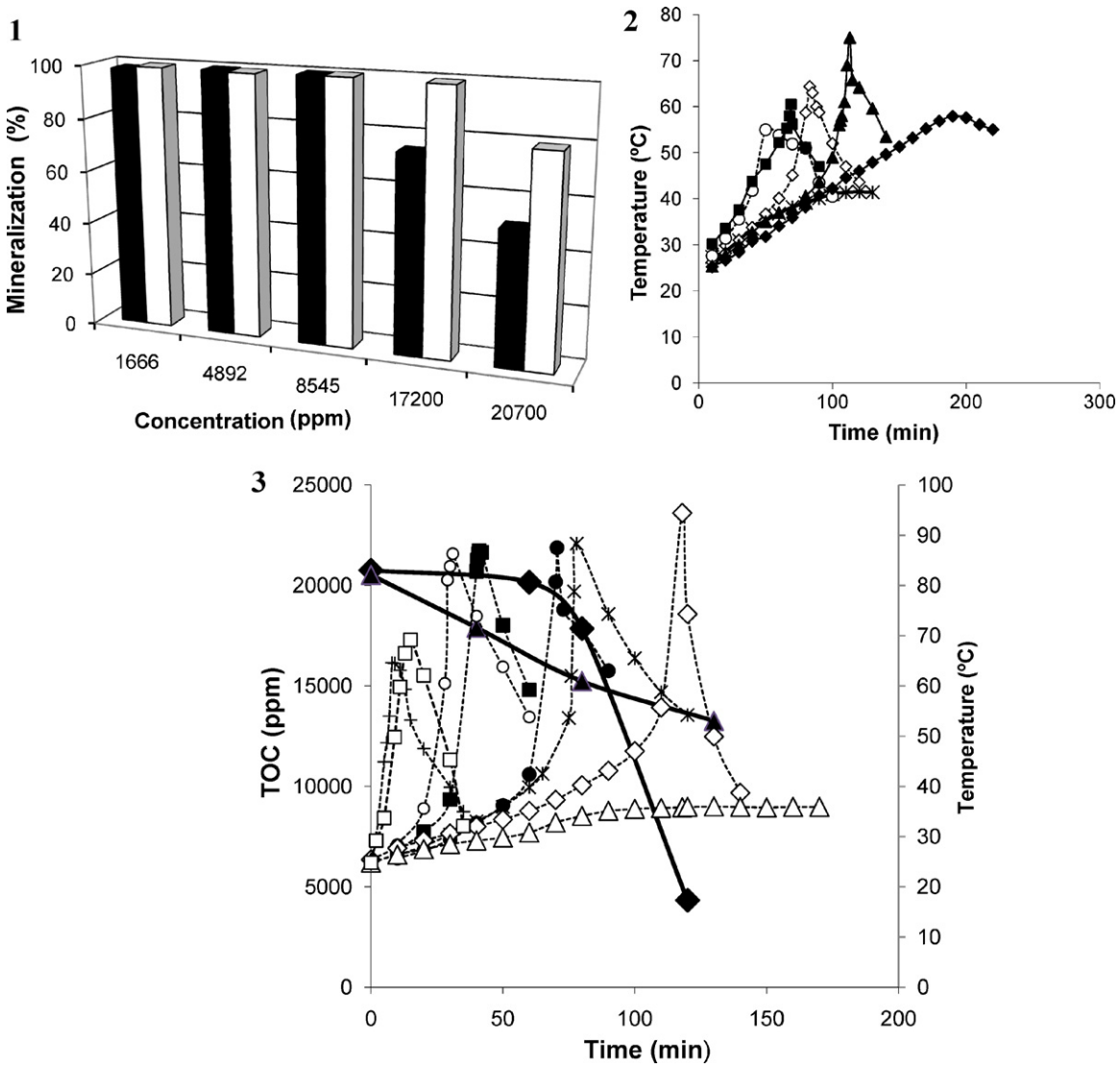

Fig. 12. (1) Mineralization of mixtures of formic–oxalic acids by photo-Fenton. [Fe^{2+}]: 200 ppm, [H_2O_2]: 60 g/L (■) and 120 g/L (□). (2) Evolution of temperature during the photo-Fenton degradation of different concentrations of formic–oxalic mixtures: 1666 ppm (○), 4892 ppm (■), 8545 ppm (◊), 17,200 ppm (▲), 20,700 ppm (♦)). [Fe^{2+}]: 200 ppm, [H_2O_2]: 60 g/L. The results for 8545 ppm with [Fe^{2+}]: 200 ppm and [H_2O_2] = 30 g/L (Ж) are also shown. (3) Evolution of temperature during the photo-Fenton degradation of different concentrations of (25:1) formic–oxalic mixtures: 1666 ppm (○), 4892 ppm (■), 8545 ppm (●), 17,200 ppm (Ж), 20,700 ppm (◊). [Fe^{2+}]: 200 ppm, [H_2O_2]: 120 g/L. The evolution of TOC for the sample with 20,700 ppm (♦) is shown. Additionally, temperature (Δ) and TOC (▲) for the same sample with 20,700 ppm but under aeration are provided. The evolution of the ΔT obtained with the Fenton treatment of formic acid alone (□) and acetic acid alone (†) (15.3 g/L each) with the same concentrations of H_2O_2 and Fe^{2+} are also illustrated.

from hydroxyl groups, in the region between 4000 and 2500 cm^{-1} are different from those of the goethite spectrum. The production of high quantities of FeOOH is expected as a result of the high ΔT observed and the fact that its formation is strongly endothermic.

3.4. Photo-Fenton of carboxylic acid mixtures

To have a better understanding of the influence of carboxylic acids on the degradation of ethylene glycol and the temperature increment observed, studies with different mixtures of the acids were performed. The concentrations of formic, acetic and oxalic acids used in this mixture were 10,500, 2750 and 3830 ppm, respectively. Fig. 11 shows the evolution of the acids during degradation ([H_2O_2]: 120 g/L, [Fe^{2+}]: 200 ppm). Their concentration is provided as carbon concentration to compare their evolution with that of TOC. No mineralization was observed with this mixture of formic, acetic and oxalic acids (Fig. 11) during the first hour of reaction (Fig. 11). Yet, the concentrations of formic and acetic acids were increased while that of oxalic was reduced. After 60 min, temperature was rapidly incremented, formic and oxalic became mineralized while the concentration of acetic acid remained constant. Several studies have shown that the acetic acid molecule is very stable [40].

After this, formic–oxalic mixtures in a 25:1 molar ratio (the one obtained in the degradation of ethylene glycol) were studied. The concentrations of TOC were varied between 1500 and 24,000 ppm and that of H_2O_2 between 60 and 120 g/L (Fig. 12 1–3). Mineralization results shown in Fig. 12 1 were obtained just after the temperature peak. Temperature evolution is shown in Fig. 12 2 and 3. The observed behavior was similar to the one with ethylene glycol and 120 g/L of H_2O_2 (Fig. 9). However, in this case ΔT was higher and occurred later, when the concentrations of acids had become increased. In all the essays, the exponential ΔT appeared when the concentration of oxalic had been greatly reduced and that of formic augmented.

In experiments with formic acid alone (15.3 g/L of TOC), H_2O_2 (120 g/L) and Fe^{2+} (200 ppm) without UV radiation, a similar ΔT was observed (Fig. 123). Nevertheless, with oxalic acid alone the ΔT appeared when its conversion to formic was almost complete. Numerous studies have shown that oxalic acid can readily form complexes with Fe^{2+} and Fe^{3+} (reactions (14)–(16)). Many of these complexes are photoactive (reaction (17)) and promote mineralization by means of reactions (18)–(23) [41,42]:

$$Fe^{3+} + C_2O_4^{2-} \leftrightarrow Fe^{III}(C_2O_4)^+ \quad (14)$$

$$Fe^{III}(C_2O_4)^+ + C_2O_4^{2-} \leftrightarrow Fe^{III}(C_2O_4)_2^- \quad (15)$$

$$Fe^{III}(C_2O_4)_2^- + C_2O_4^{2-} \leftrightarrow Fe^{III}(C_2O_4)_3^{3-} \quad (16)$$

$$Fe^{III}(C_2O_4)_n^{3-2n} + h\nu \rightarrow Fe^{2+} + (n-1)C_2O_4^{2-} + C_2O_4^{\bullet-} \quad (17)$$

$$C_2O_4^{\bullet-} \rightarrow CO_2 + CO_2^{\bullet-} \quad (18)$$

$$CO_2^{\bullet-} + O_2 \rightarrow CO_2 + O_2^{\bullet-} \quad (19)$$

$$Fe^{3+} + O_2^{\bullet} \rightarrow Fe^{2+} + O_2 \quad (20)$$

$$Fe^{III}(C_2O_4)_n^{3-2n} + O_2^{\bullet-} \rightarrow O_2 + Fe^{II}(C_2O_4)_n^{2-2n} \quad (21)$$

$$Fe^{III}(C_2O_4)_n^{3-2n} + HO_2^{\bullet} \rightarrow O_2 + Fe^{II}(C_2O_4)_n^{2-2n} \quad (22)$$

$$Fe^{II}(C_2O_4) + H_2O_2 \rightarrow Fe^{III}(C_2O_4)^+ + {}^{\bullet}OH + OH^- \quad (23)$$

The obtained results have shown that the reaction of formic and/or acetic acids with Fe^{2+} and H_2O_2 (in the concentrations here employed) is responsible for the ΔT and mineralization achieved. The degradation of formic acid through $^{\bullet}OH$ radical attack to yield the radical $HCOO^{\bullet}$ has been described by reaction (24). This radical can react with H_2O_2 (reaction (25)) to regenerate formic acid or with oxygen (reaction (26)) to become mineralized.

$$HCOOH + {}^{\bullet}OH \rightarrow HCOO^{\bullet} + H_2O \quad (24)$$

$$H\text{–}COO^{\bullet} + H_2O_2 \rightarrow HCOOH + HO_2^{\bullet} \quad (25)$$

$$H\text{–}COO^{\bullet} + O_2 \rightarrow HO_2^{\bullet} + CO_2 \quad (26)$$

In this work, formic acid was mineralized after the exponential ΔT. This means that reaction (26) was not favored and, as stated above reaction (25) would cause the temperature peak. To confirm this hypothesis, the same experiments (20,700 ppm of mixture formic: oxalic acid 25:1, 120 g/L H_2O_2) have been performed but aerating the reactor (100 mL/min) to favor reaction (26). Under these conditions, ΔT was very low and mineralization was progressive (Fig. 123). This means that the reaction of dissolved oxygen with $HCOO^{\bullet}$ radicals (reaction (26)) inhibits reaction (25) responsible for ΔT.

The degradation by photo-Fenton of ethylene glycol under aeration was also performed (Fig. 9) and the resulting ΔT was notably slower than without aeration. In these reactions, formic acid could be forming a complex with FeOOH as the one detected in the FTIR studies. The existence of organic complexes with goethite that promote degradation has already been proposed [43].

As indicated above, oxalic acid can readily form complexes with Fe^{2+} and/or Fe^{3+}. Thus, while the acid is present in solution at the adequate concentrations, reactions (14)–(16) are prevalent. This would explain the slowing down of the Fenton reactions illustrated in Figs. 2 and 4.

Furthermore, in this work numerous experiments have been performed with elevated concentrations of ethylene glycol or carboxylic acids at different concentrations of H_2O_2. For these experiments, the achieved mineralization was plotted versus the mol/mol $[H_2O_2]$/TOC ratio (Fig. 13). As can be observed, total mineralization was achieved when the ratio value tended to 3. This means that 3 mol of H_2O_2 are needed to mineralize 1 mol of organic carbon to CO_2, in other words, the implication of reactions (1), (3) and (25).

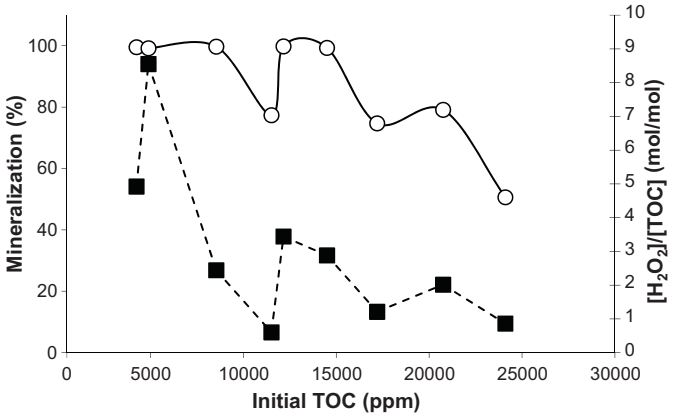

Fig. 13. Mineralization (○) and $[H_2O_2]$/TOC ratio (■) versus initial TOC for the degradation of ethylene glycol and carboxylic acid mixtures by photo-Fenton.

4. Conclusions

The present work describes, to our knowledge for the first time, the degradation mechanism of high concentrations of ethylene glycol by photo-Fenton. The main conclusions are the following:

- The Fenton reaction with high concentrations of H_2O_2 and formic acid (and/or acetic) generates a strong temperature increment that promotes the almost complete mineralization of highly concentrated solutions in about 5 min.
- The main reactions involved in the process are: Fenton reaction (1), the formation of goethite (3), the reaction of $RCOO^{\bullet}$ radicals (formed from formic and/or acetic acids) with H_2O_2. The latter is proposed as responsible for the temperature increment observed.
- The process previously described is controlled by the formation of Fe–oxalate complexes that slow down the temperature increment and mineralization.
- The Fe–formiate complexes identified by FTIR can be involved in the process.
- The strong temperature increment that occurs at the end of the process causes the precipitation of iron as goethite.
- Exothermic processes such as those determined in the present study can open new research lines for the treatment of real, highly concentrated samples.

Acknowledgment

We are grateful for the funding of the Spanish Ministry of Science and Innovation for their financial support through the Project CTQ2008-05961-C02-02, CTQ2008-05961-C02-01

References

[1] H.J.H. Fenton, J. Chem. Soc. 65 (1894) 899–910.
[2] Ch. Walling, Acc. Chem. Res. 8 (1975) 125–131.
[3] C. Walling, A. Goosen, J. Am. Chem. Soc. 95 (1973) 2987–2991.
[4] C. Lee, J. Yoon, Chemosphere 56 (2004) 923–934.
[5] J.A. Giroto, A.C.S.C. Teixeira, C.A.O. Nascimento, R. Guardani, Chem. Eng. Process. 47 (2008) 2361–2369.
[6] I.B.S. Will, J.E.F. Moraes, A.C.S.C. Teixeira, R. Guardani, C.A.O. Nascimento, Sep. Purif. Technol. 34 (2004) 51–57.
[7] A. López, M. Pagano, A. Volpe, A.C. Di Pinto, Chemosphere 54 (2004) 1005–1010.
[8] M. Pérez, F. Torrades, J.A. García-Hortal, X. Domènech, J. Peral, Appl. Catal. B: Environ. 36 (2002) 63–74.
[9] M. Perez, F. Torrades, X. Domènech, J. Peral, Water Res. 36 (2002) 2703–2710.
[10] E. Cokay Catalkaya, F. Kargi, J. Hazard. Mater. B139 (2007) 244–253.
[11] A.M.F.M. Guedes, L.M.P. Madeira, R.A.R. Boaventura, Water Res. 37 (2003) 3061–3069.
[12] H. Tekin, O. Bilkay, S.S. Ataberk, T.H. Balta, I.H. Ceribasi, F.D. Sanin, F.B. Dilek, U. Yetis, J. Hazard. Mater. B136 (2006) 258–265.

[13] N.S.S. Martínez, J. Fíguls Fernández, X. Font Segura, A. Sánchez Ferrer, J. Hazard. Mater. B101 (2003) 315–322.
[14] P. Bautista, A.F. Mohedano, M.A. Gilarranz, J.A. Casas, J.J. Rodriguez, J. Hazard. Mater. 143 (2007) 128–134.
[15] Y. Lee, C. Lee, J. Yoon, Chemosphere 51 (2003) 963–971.
[16] A. Santos, P. Yustos, S. Rodriguez, E. Simon, F. Garcia-Ochoa, J. Hazard. Mater. 146 (2007) 595–601.
[17] K. Dutta, S. Mukhopadhyay, S. Bhattacharjee, B. Chaudhuri, J. Hazard. Mater. B 84 (2001) 57–71.
[18] L. Lunar, D. Sicilia, S. Rubio, D. Perez-Bendito, U. Nickel, Water Res. 34 (6) (2000) 1791–1802.
[19] F.J. Rivas, F.J. Beltrán, J.F. Garcia-araya, V. Navarrete, O. Gimeno, J. Hazard. Mater. B91 (2002) 143–157.
[20] C. Lee, D.L. Sedlak, J. Mol. Catal. A: Chem. 311 (2009) 1–6.
[21] G.K.B. Lopes, H.M. Schulman, M. Hermes-Lima, Biochim. Biophys. Acta 1472 (1999) 142–152.
[22] W. Feng, D. Nansheng, Chemosphere 41 (2000) 1137–1147.
[23] J. Araña, E. Tello Rendón, J.M. Doña Rodríguez, J.A. Herrera Melián, O. González Díaz, J. Pérez Peña, Chemosphere 44 (2001) 1017–1023.
[24] R.D. Sills, P.A. Blakeslee, Chemical Deicers and the Environment, Lewis Publishers, Boca Raton, FL, 1992, pp. 323–340.
[25] SRI Directory of chemical producers—United States of America, Menlo Park, CA, Stanford Research Institute International, 1993, p. 598, 890.
[26] B. Dietrick McGinnis, V. Dean Adamas, E.J. Middlebrook, Water Res. 34 (2000) 2346–2354.
[27] B. Dietrick McGinnis, V. Dean Adamas, E.J. Middlebrook, Chemosphere 45 (2001) 101–108.
[28] APHA, Standard Methods for the Examination of Water and Wastewater, 21st ed., APHA, Washington, DC, USA, 2005.
[29] S. Dobson, Ethylene glycol: Environmental aspects, I. International Programme on Chemical Safety II. Series, ISBN 92 4 153022 7 (NLM Classification: QD 305.A4), ISSN 1020-6167.
[30] T.J. Hardwick, Can. J. Chem. 35 (1957) 428–436.
[31] C.-S. Chiou, Y.-H. Chen, C.-T. Chang, C.-Y. Chang, J.-L. Shie, Y.-S. Li, J. Hazard. Mater. B135 (2006) 344–349.
[32] R. Chen, J.J. Pignatello, Environ. Sci. Technol. 31 (1997) 2399–2406.
[33] H. Christensen, K. Sehested, H. Corfitzen, J. Phys. Chem. 86 (1982) 1588–1590.
[34] H. Christensen, K. Sehested, Radiat. Phys. Chem. 18 (1981) 723–731.
[35] D.D. Dionysiou, M.T. Suidan, I. Baudin, J.-M. Laıné, Appl. Catal. B: Environ. 50 (2004) 259–269.
[36] A.J. Elliot, D.R. McCracken, G.V. Buxton, N.D. Wood, J. Chem. Soc. Faraday Trans. 86 (9) (1990) 1539–1547.
[37] A. Sinha, S. Chakrabarti, B. Chaudhuri, S. Bhattacharjee, P. Ray, S.B. Roy, Ind. Eng. Chem. Res. 46 (2007) 3101–3107.
[38] M.D. Caki, G.S. Nikoli, L.A. Ili, Bull. Chem. Technol. Maced. 21 (2002) 135–146.
[39] J. Araña, O. González Díaz, M. Miranda Saracho, J.M. Doña Rodríguez, J.A. Herrera Melián, J. Pérez Peña, Appl. Catal. B: Environ. 32 (2001) 49–61.
[40] R.J. Bigda, Chem. Eng. Prog. 91 (12) (1995) 62–66.
[41] J. Jeong, J. Yoon, Water Res. 38 (2004) 3531–3540.
[42] J. Jeong, J. Yoon, Water Res. 39 (2005) 2893–2900.
[43] J. He, W. Ma, W. Song, J. Zhao, X. Qian, S. Zhang, Jimmy C. Yu., Water Res. 39 (2005) 119–128.